Environmental Modelling & Software 24 (2009) 411–422

Contents lists available at ScienceDirect

Environmental Modelling & Software

journal homepage: www.elsevier.com/locate/envsoft

A GIS-based tool for modelling large-scale crop-water relations

Junguo Liu*

Eawag, Swiss Federal Institute of Aquatic Science and Technology, Ueberlandstrasse 133, 8600 Dübendorf, Switzerland

ARTICLE INFO

Article history:
Received 25 May 2008
Received in revised form 6 August 2008
Accepted 14 August 2008
Available online 17 October 2008

Keywords:
Crop water productivity
EPIC
GEPIC
Wheat
Maize
Rice

ABSTRACT

Recent research on crop-water relations has increasingly been directed towards the application of locally acquired knowledge to answering the questions raised on larger scales. However, the application of the local results to larger scales is often questionable. This paper presents a GIS-based tool, or a GEPIC model, to estimate crop water productivity (CWP) on the land surface with spatial resolution of 30 arc-min. The GEPIC model can estimate CWP on a large-scale by considering the local variations in climate, soil and management conditions. The results show a non-linear relationship between virtual water content (or the inverse of CWP) and crop yield. The simulated CWP values are generally more sensitive to three parameters, i.e. potential harvest index for a crop under ideal growing conditions (HI), biomass-energy ratio indicating the energy conversion to biomass (WA), and potential heat unit accumulation from emergence to maturity (PHU), than other parameters. The GEPIC model is a useful tool to study crop-water relations on large scales with high spatial resolution; hence, it can be used to support large-scale decision making in water management and crop production.

Software availability

Name of software: GEPIC
Program language: Visual Basic for Applications (VBA), ArcObject
Developer: Swiss Federal Institute of Aquatic Science and Technology (Eawag)
Contact address: Swiss Federal Institute of Aquatic Science and Technology (Eawag), Ueberlandstrasse 133, CH-8600, Duebendorf, Switzerland
Software required: ArcGIS 9.1
Availability: can be made available to researchers on request to the author.

1. Introduction

Water is indispensable for crop production. Dependence on water comes from the intrinsic process of crop growth. This process requires carbon dioxide (CO_2), and exposes a plant's interior to the drying power of the atmosphere (Holbrook and Zwieniecki, 2003). When plants absorb less water through their roots than is transpired from their leaves, water stress develops. As a result, stomatal pores in the leaf surface progressively close (Lauer and Boyer, 1992; Lawlor, 1995). This stomatal closure not only decreases the rate of transpiration (Gimenez et al., 1992; Lauer and Boyer, 1992; Ort et al., 1994), but also reduces photosynthetic assimilation of CO_2, posing constraints on plant growth (Lauer and Boyer, 1992; Quick et al., 1992; Ort et al., 1994). Water stress substantially alters plant's metabolism, decreases plant growth and photosynthesis and profoundly affects ecosystems and agriculture, and thus human societies (Lawlor, 1995; Evans, 1998; Tezara et al., 1999).

Defined as the ratio of crop yield to crop evapotranspiration, crop water productivity (CWP) combines two important and interrelated processes in agricultural systems, and it is an important indicator for measuring the quantitative relations between crop production and water consumption (Liu et al., 2007a,b). Another concept, virtual water content (VWC), has recently been introduced to express the amount of water consumed in terms of evapotranspiration to produce a unit of crop product (Hoekstra and Hung, 2005). VWC is the inverse of CWP. Recent efforts in CWP and VWC studies are increasingly being directed towards the application of knowledge acquired on small spatial scales to answering questions raised on larger scales. Zwart and Bastiaanssen (2004) review local measurements of CWP from 84 literature sources and discuss general patterns of CWP in relation to climate, irrigation and soil nutrient management on a global scale. Hoekstra and Hung (2005) calculate the values of VWC based on the climate station data in the capital city of individual countries, and then quantify the volumes of virtual water flows among nations through international crop trade. Rockström et al. (2007) develop a CWP function based on a number of empirical field observations of grains in both tropical and temperate environments, and assess the water challenge of attaining the 2015 hunger targets in 92 developing

* Corresponding author. Tel.: +41 448235012; fax: +41 448235375.
E-mail addresses: junguo.liu@eawag.ch, water21water@yahoo.com

1364-8152/$ – see front matter © 2008 Elsevier Ltd. All rights reserved.
doi:10.1016/j.envsoft.2008.08.004

countries set out in the United Nations Millennium Development Goals. It needs to be pointed out that the locally valid findings may not be representative of other locations, and the application of the local results to larger scales is questionable. There is an increasing need for a new research tool that is capable of studying large-scale crop-water relations, and that considers, in the mean time, local variations.

Previously, several models have been developed to study food production on large scales. Some of the models regard water as an influencing factor in crop production. In this paper, the large-scale food production models are first reviewed. Their advantages and disadvantages in studying crop-water relations are emphasized. Then, a GEPIC model is introduced as an effective tool for conducting a global crop-water relation study. The model is applied to estimate the CWP of three major cereal crops (wheat, maize and rice) on a global scale, and the results are compared with other studies.

2. Large-scale food production models

In the literature, models applied in food production studies on global and national scales mainly fall into six major categories: physical models, economic models, physical-economic models, time series models, regression analysis models, and integrated models. An overview of these models is presented below, and the summary is given in Table 1. Two issues are emphasized here, namely the ability to study crop-water relations, and spatial resolution.

Crop growth models are a type of commonly used physical model. Crop growth models often simulate crop growth with some empirical functions or model the underlying physiological processes of crop growth in relation to the surrounding environment. A number of crop growth models have been developed and widely used, such as EPIC (Williams et al., 1989), DSSAT (IBSNAT, 1989), WOFOST (Hijmans et al., 1994), CropSyst (Stockle et al., 1994), YIELD (Burt et al., 1981), CropWat (Clarke et al., 1998) and CENTRURY (Parton et al., 1992). Most existing crop growth models are mainly used for point or site specific applications (Priya and Shibasaki, 2001; Liu et al., 2007b). Crop growth models are rarely used alone for food production studies on a global or national scale. However, combining crop growth models with other techniques is a common way to extend the applicability of these models for large-scale studies, which will be introduced later. The Agro-ecological Zones (AEZ) approach is another example of the physical model. The AEZ approach uses a land resources inventory to assess all feasible agricultural land-use options for specific management conditions and levels of inputs, and to quantify the expected production of relevant cropping activities (Fischer et al., 2002). The AEZ approach can provide answers to what-if scenarios such as establishing what the global food production is if there are high levels of water inputs. A major drawback is that the levels of irrigation inputs can be set only as low, medium and high. It is impossible to make good quantifications; hence, the quantitative analysis of crop-water relations is difficult to achieve.

The World Food Model developed by the Food and Agriculture Organization of the United States (FAO) is a typical economic model to simulate and project global food production. This model is a price-equilibrium, multi-commodity model, and it is designed to provide year-by-year world price-equilibrium solutions for 40 agricultural products (Frohberg and Britz, 1994). In this model, the main components are the supply and demand equations, and the market clearing mechanism. Only the economic factor, or price, is considered for global food production; all other equally important factors, including water, are ignored.

The IMPACT model (International Model for Policy Analysis of Agricultural Commodities and Trade) is a typical example of the physical-economic model. This model examines the effects of various food policies, the impact of different rates of agricultural research investment on crop productivity, and the impact of income and population growth on long-term food demand and supply balances and food security (Rosegrant et al., 2001). The model comprises a set of 36 country or regional sub-models, each determining supply, demand, and prices for 32 agricultural commodities. The country and regional agricultural sub-models are linked through trade. In light of the importance of water for food production, the IMPACT-WATER model was developed to integrate the IMPACT model with a Water Simulation Model (Rosegrant et al., 2002). The IMPACT-WATER model uses a finer disaggregation of 69 river basins in recognition of the fact that significant climate and hydrologic variations within regions make the use of large spatial

Table 1
Overview of the conventional model approaches for the study of food production on global or national scales

Model type	Typical examples	Inputs	Spatial resolution	Scale	Major shortcomings
1.Physical model	1.1 Crop growth models[a]	Climate, soil, land, irrigation, fertilizer etc.	Local	Site	Point or site-specific application
	1.2 Agro-ecological zones (AEZ)	Climate, soil, land, irrigation, fertilizer etc.	30 arc-minutes	Global	No quantification of irrigation and fertilizer; seperate consideration of soil and climate
2. Economic model	2.1 FAO World Food Model	Price	National	Global	Only price is considered the influencing factor
3. Physical-economic model	3.1 IMPACT	Food policy, research investment, income, price	Regional or national	Global	Low spatial resolution; no consideration of water, fertilizer, soil nutrient and land-use
	3.2 IMPACTWATER	Food policy, research investment, income, price, water	Regional or national	Global	Low spatial resolution; no consideration of fertilizer, soil nutrient and land-use
4. Time series model	4.1 Linear yield growth model	Yield growth rate, time	Regional or national	Global or national	Poor accuracy; lack of ability to analyze the impacts of irrigation and fertilizer on crop production
5. Regression analysis model	5.1 Yield as a function of influencing factors	Precipitation, irrigation, fertilizer, GDP, latitude (one or many of them)	Regional or national	Global or national	Poor accuracy, low spatial resolution
6. Integrated model	6.1 Crop growth model + regression	Climate, soil, land, management	Regional or national	Global or national	Whether yield function derived from reference sites can be extrapolated to other locations is uncertain
	6.2 Crop growth model + GIS	Climate, soil, land, management	30 arc-min or even higher	Global or national	Development and application have a recent origin

[a] Crop growth models alone are rarely used for studies on global or national scales. They are presented in the table because they are often applied in the integrated models.

units inappropriate for water resource assessment and modelling. For both the IMPACT and IMPACT-WATER models, the assessments conducted on the national or regional scale disguise spatial variations within a country or region.

The time series methods assume that yield is a function of time and yield growth rate (Doos and Shaw, 1999; Dyson, 1996; Tweeten, 1998). Linear yield growth models are constructed to estimate the yield growth rates with past yield trends. Then the yield growth rates experienced in history were used to project the regional or national yield in the future (Dyson, 1999). The PODIUM model developed by the International Water Management Institute (IWMI) takes this approach. PODIUM projects national food production based on expected yields and cultivated area under both irrigated and rainfed conditions (Seckler et al., 1998). The yield and cultivated area in the future are based on past trend, or user-defined scenarios. The time series models consider no other influencing factors such as irrigation or fertilizer application rates; hence, they are unable to analyze the impacts of these factors on crop production. In addition, low accuracy limits the application of the time series methods (Tan and Shibasaki, 2003).

For regression analysis models, regression equations are developed from observed data to link crop yield to several influencing factors such as precipitation, temperature, irrigation or fertilizer (Rosenzweig et al., 1999). The crop-water relation can be analyzed when the regression analysis is conducted between crop yield and water-related variables such as precipitation and irrigation. Here accuracy is the limiting factor (Tan and Shibasaki, 2003).

There are studies integrating crop growth models with regression analysis. Statistical analyses are used to derive agro-climatic regional yield transfer functions from previously simulated site-level results (Rosenzweig and Iglesias, 1998; Parry et al., 1999; Rosenzweig et al., 1999; Iglesias et al., 2000). The yield transfer functions can include the influencing factors of precipitation and irrigation. These functions are then applied to the spatial input data to estimate crop yield in different locations. It remains to be seen whether the transfer function derived from one geographic location can be extrapolated to other locations.

Integrating crop growth models with a Geographic Information System (GIS) is another type of integrated model. Combined with the powerful function of spatial data storage and management in a GIS, a crop growth model may be extended to address spatial variability of yield as affected by climate, soil, and management factors. There have been some preliminary attempts to integrate crop growth models with a GIS (Curry et al., 1990; Rao et al., 2000; Priya and Shibasaki, 2001; Ines et al., 2002; Stockle et al., 2003), and these attempts mainly focus on scales no higher than national ones. Recent research has integrated the EPIC model with a GIS for global-scale studies (Tan and Shibasaki, 2003; Liu et al., 2007a,b). In this paper, the GEPIC model developed in the Swiss Federal Institute of Aquatic Science and Technology is introduced, and it is applied to simulate CWP of wheat, maize and rice.

3. Description of the GEPIC model

3.1. Framework of the GEPIC model

GEPIC is a GIS-based crop growth model integrating a bio-physical EPIC model (Environmental Policy Integrated Climate) with a GIS to simulate the spatial and temporal dynamics of the major processes of the soil–crop–atmosphere-management system (Liu et al., 2007a,b). The general idea of the GEPIC model is expressed in Fig. 1. The EPIC model is designed to simulate crop-related processes for specific sites with site-specific inputs. By integrating EPIC with a GIS, the GEPIC model treats each grid cell as a site. It simulates the crop-related processes for each predefined grid cell with spatially distributed inputs. The inputs are provided to the model in terms of GIS raster maps as well as text files. Necessary maps include land-use maps, elevation and slope maps, irrigation maps, fertilizer maps, climate code maps, and soil code maps. The land-use maps provide information on crop distribution (code 0 indicates absence of a specific crop, while 1 and 2 indicate existence of the crop under rainfed and irrigated conditions, respectively). The elevation and slope maps show the average elevation and slope in each grid cell. The irrigation and fertilizer maps show the annual maximum irrigation depth and fertilizer application rate. The climate and soil code maps indicate the code numbers of the climate and soil files in each grid cell. These code numbers correspond to the text files of climate and soil data. Climate files contain daily weather data (e.g. daily precipitation, daily minimum and maximum temperatures) and monthly weather statistics. Soil files contain several soil parameters (e.g. soil depth, percent sand and silt, pH, organic carbon content, etc). Annual irrigation and fertilizer inputs are provided in the irrigation and fertilizer maps. The outputs of the GEPIC model are raster GIS maps representing the spatial distribution of output variables such as crop yield and evapotranspiration.

To develop such a GIS-based crop growth model, the ESRI's GIS software ArcGIS 9.1 was selected mainly due to its wide application. The well-documented ArcObjects libraries were also an important reason for the selection. The ArcObjects libraries allow any available function of ArcGIS to be exploited. In addition, the functionality can be further extended by using third-party Component Object Model-compliant (COM-compliant) programming languages such as Visual Basic, C++, Java, or Python (ESRI, 2004). Visual Basic for Applications (VBA) in ArcGIS were used to develop the GEPIC model mainly due to two reasons. First, VBA is a built-in language within ArcGIS. The use of VBA requires no external development environment. Second, nowadays online forum has become an effective way for program developers to seek similar solutions to complex programming problems. While the solutions are similar in many COM-compliant languages, most solutions are provided in online forums in the Visual Basic context (Stevens et al., 2007).

In the GEPIC model, ArcGIS is used as an application framework, input editor, and map displayer. As an application framework, ArcGIS provides the main programming language VBA to design the interface of GEPIC, and to design programs for input data access, text output data generation, and output map creation. As an input editor, ArcGIS is used to convert vector input data into raster data, which are the main input format. One typical example is the climate data. Daily climate data are often available for various stations, while the code of each station is presented as attributed point data. The point data is converted into raster data with a method of Thiessen Polygons, with which the daily climate data from the closest climate station is used as a representative for a grid cell (Liu et al., 2007b). As a map displayer, ArcGIS can be used to visualize the GIS data (e.g. vector or raster input data; raster output data etc).

The GEPIC software comprises three components. The most obvious component is the proprietary GIS, which is a standard ArcMap window in ArcGIS 9.1. The least obvious component is the EPIC model, which is the core of all simulations. The third component is the GEPIC interface (see Fig. 2), and it links GIS and EPIC. The interface contains toolbars and menus. The toolbars provide functional buttons to locate raster input data sets, to select the simulated area and crops, and to specify spatial resolution, and to set the locations of the EPIC file, and input and output files. It further provides buttons to edit inputs into EPIC required input files, to run the EPIC model, and to generate output maps. The menu has submenus, which allow users to perform the same tasks as the toolbars.

3.2. The crop growth model

Crop growth is simulated with a daily time step by modelling leaf area development, light interception, and conversion of intercepted light into biomass. The daily potential increase in biomass is estimated with Monteith's approach (Monteith, 1977):

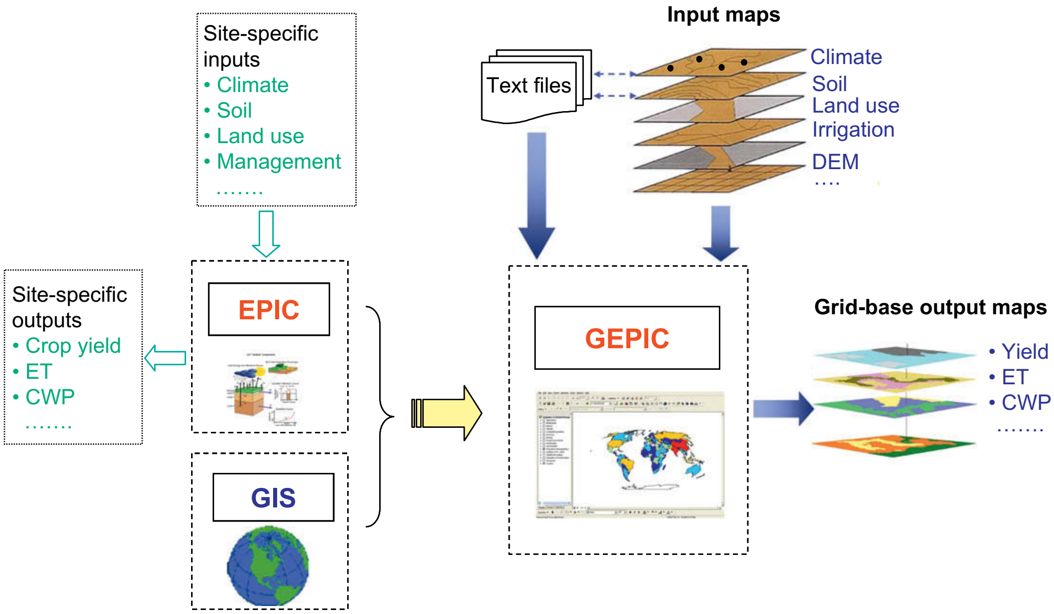

Fig. 1. General framework of the GEPIC model.

$$\Delta B_{p,i} = 0.001 \times \mathrm{WA} \times \mathrm{PAR}_i \tag{1}$$

where ΔB_p is daily potential increase in biomass in kg ha^{-1} in day i, WA is a biomass-energy ratio indicating the energy conversion to biomass in (kg ha^{-1})(MJ m^{-2})$^{-1}$, PAR is intercepted photosynthetic active radiation in MJ m^{-2} d^{-1}, and it is estimated with Beer's law equation (Monsi and Saeki, 1953) as follows:

$$\mathrm{PAR}_i = 0.5\mathrm{RA}_i\left(1 - e^{-0.65\mathrm{LAI}_i}\right) \tag{2}$$

Where RA is solar radiation in MJ m^{-2}, LAI is the leaf area index, and the constant 0.5 is used to convert solar radiation to photosynthetically active radiation.

The potential biomass is adjusted daily if any of the five stress factors (water stress, temperature stress, nitrogen stress, phosphorus stress and aeration stress) is less than 1.0 using the equation

$$\Delta B_{a,i} = \Delta B_{p,i}\gamma_{\mathrm{reg},i} \tag{3}$$

where ΔB_a is the daily actual increase in biomass in kg ha^{-1}, and γ_{reg} is the crop growth regulation factor, which is the minimum of the

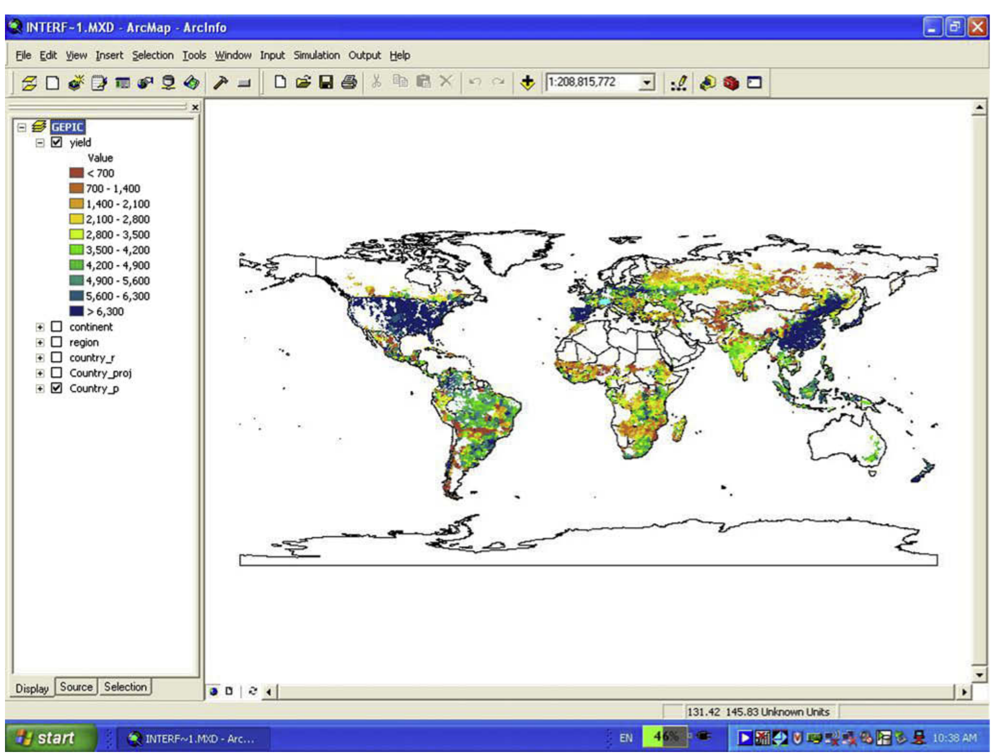

Fig. 2. Interface of the GEPIC software.

above five stress factors. Details for estimate γ_{reg} can be found in Williams et al. (1989).

Above-ground biomass on the day of harvest is calculated as the sum of the daily actual increase in biomass in growing season:

$$B_{AG} = \sum_{i=1}^{N} \Delta B_{a,i} \tag{4}$$

where B_{AG} is the above-ground biomass on the day of harvest in kg ha^{-1}, N is the number of days from planting date to harvest date.

Crop yield is estimated using the harvest index concept:

$$\mathrm{YLD} = \mathrm{HIA} \times B_{AG} \tag{5}$$

where YLD is the amount of economic dry yield that could be removed from the field in kg ha^{-1}, and HIA is the water stress adjusted harvest index. For non-stressed conditions, the harvest index increases non-linearly from zero at planting to the potential harvest index at maturity. The harvest index is reduced by water stress using the following equation (Williams et al., 1989):

$$\mathrm{HIA}_i = \mathrm{HIA}_{i-1} - \mathrm{HI}\left(1 - \frac{1}{1 + \mathrm{WSYF} \times \mathrm{FHU}_i(0.9 - \mathrm{WS}_i)}\right) \tag{6}$$

where HI is the potential harvest index on the day of harvest, WSYF is a crop parameter expressing the sensitivity of harvest index to drought, FHU is a crop growth stage factor, and WS is the water stress factor, and subscript i and $i-1$ are the Julian days of the year.

3.3. Soil evaporation and crop transpiration

Reference evapotranspiration is simulated as a function of extraterrestrial radiation and air temperature with Hargreaves method (Hargreaves and Samani, 1985):

$$\lambda \mathrm{ET}_0 = 0.023 H_0 (T_{\mathrm{mx}} - T_{\mathrm{mn}})^{0.5} (T_{\mathrm{av}} + 17.8) \tag{7}$$

whereλ is the latent heat of vaporization in MJ kg^{-1}, ET_0 is the reference evapotranspiration in mm d^{-1}, H_0 is the extraterrestrial radiation in MJ m^{-2} d^{-1}, T_{mx}, T_{mn}, and T_{av} are the maximum, minimum and mean air temperature for a given day in °C.

Evaporation from soil and transpiration from plants are calculated separately by an approach similar to that of Ritchie (1972). Potential transpiration is simulated as a linear function of ET_0 and leaf area index (LAI).

$$T_{\mathrm{p}} = \mathrm{ET}_0 \mathrm{LAI}/3 \quad 0 < \mathrm{LAI} < 3 \tag{8}$$

$$T_{\mathrm{p}} = \mathrm{ET}_0 \quad \mathrm{LAI} \geq 3 \tag{9}$$

where T_{p} is the potential transpiration in mm d^{-1}, and LAI is the leaf area index.

Potential evaporation is simulated with Eq. (10):

$$E_{\mathrm{p}} = \max\{(\mathrm{ET}_0 - I)\lambda_s,\ 0\} \tag{10}$$

where E_{p} is the potential soil evaporation in mm d^{-1}, I is the rainfall interception in mm d^{-1}, and λ_{s} is a soil cover index.

When $\mathrm{ET}_0 < I$, the actual plant transpiration (T_{a}) and soil evaporation (E_{a}) are set to zero. Otherwise, they are calculated as follows:

$$T_{\mathrm{a}} = \min\{\mathrm{ET}_0 - I, T_{\mathrm{p}}\} \tag{11}$$

$$E_{\mathrm{a}} = \min\{E_{\mathrm{p}}, E_{\mathrm{p}}(\mathrm{ET}_0 - I)/(E_{\mathrm{p}} + T_{\mathrm{a}})\} \tag{12}$$

The actual evapotranspiration (ET_{a}) is the sum of actual soil evaporation and crop transpiration.

3.4. Sensitivity analysis

There are several methods to perform sensitivity analysis. These methods range from the quantitative sampling-based methods to other forms of global sensitivity with regional properties, down to the simplest class of the One Factor At a Time (OAT) screening techniques (Campolongo et al., 2007). The most commonly used method is sampling-based. Sampling-based sensitivity analysis is one in which the model is executed repeatedly for a large number of parameter combinations, in which parameter values are sampled from a certain distribution of the parameters. Although commonly used, the method is not practical here due to high computing costs. For sampling-based sensitivity analysis, the number of parameter combinations should be relatively large (approximately 500–1000). In this study, over 15,000 simulations are performed for each crop (i.e. 25,783 for wheat, 26,896 for maize, and 15,796 for rice) on a global scale for one set of parameter combinations. To reduce computation load, algebraic sensitivity analysis is proposed to find algebraically the sensitivities of output to variations in contributing factors (Norton, 2008). However, the results of the algebraic sensitivity analysis often become too complicated to derive and interpret as more equations are analyzed (Norton, 2008). This shortcoming limits the application of the algebraic sensitivity analysis to the GEPIC model, which consists of several interrelated complex components, such as crop growth component, hydrological component and nutrient cycle component. Each of the components includes several equations (the main equations used for the calculation of crop growth and crop evapotranspiration are described in Section 3.2 and 3.3). For practical reasons, the simplest method, or the OAT method, is applied to examine the relative sensitivity of CWP to several important parameters. In the OAT method only one factor, X_i, varies at a time while other factors are fixed. The change in model output can then be unambiguously attributed to such a change in factor X_i. A relative sensitivity index, defined as the ratio between the relative normalized change in output to the normalized change in related input, was calculated to indicate the magnitude of the sensitivity of the model output to the input factors (Brunner et al., 2004). The relative sensitivity index S in Eq. (13) developed by McCuen (1973) was slightly modified (Eq. (14)) to consider the absolute change in model output and related input (Wang et al., 2005b):

$$S = \frac{\Delta Y}{\Delta X}\frac{X}{Y} \tag{13}$$

$$S_i = \frac{|Y(X_1, \ldots, X_i + \Delta X_i, \ldots X_p) - Y(X_1, \ldots, X_i, \ldots X_p)|}{Y(X_1, \ldots, X_i + \Delta X_i, \ldots X_p)} \frac{X_i}{|\Delta X_i|} \tag{14}$$

where S_i is a sensitivity index indicating the relative partial effect of parameter X_i on model output Y, p is the total number of parameters considered, and Y is the model output (i.e. CWP in this study), $\triangle X$ is a small change in X, $\triangle Y$ is the change in Y in response to the change in X.

The selection of important parameters that are closely related to CWP is mainly based on literature review and expert judgment. The simulation of CWP depends on the simulation of two processes: crop yield and crop evapotranspiration. Wang et al. (2005a) reported that the following six parameters are the most important for the related processes: biomass-energy ratio (WA), potential harvest index (HI), potential heat unit (PHU), water stress-harvest index (PARM3), SCS curve number index coefficient (PARM42), and the difference in soil water contents at field capacity and wilting point (DIFFW). DIFFW is not used for sensitivity analysis in this paper because it is not a parameter directly used in the EPIC model. In this study, the sensitivity of CWP to all the other five parameters is analyzed. For each grid cell, CWP is first calculated with default parameter values; then, CWP is simulated by increasing and decreasing the default parameter values by 10%. Based on Eq. (14), two values of the sensitivity index are calculated for each of the five parameters in each grid cell. We present the average of these two values as follows:

$$\overline{S}_i = \frac{1}{2}\left(\frac{\left|\mathrm{CWP}_{1.1X_i} - \mathrm{CWP}_{X_i}\right|}{0.1\mathrm{CWP}_{X_i}} + \frac{\left|\mathrm{CWP}_{0.9X_i} - \mathrm{CWP}_{X_i}\right|}{0.1\mathrm{CWP}_{X_i}}\right) = \frac{\left|\mathrm{CWP}_{1.1X_i} - \mathrm{CWP}_{X_i}\right| + \left|\mathrm{CWP}_{0.9X_i} - \mathrm{CWP}_{X_i}\right|}{0.2\mathrm{CWP}_{X_i}} \quad (15)$$

where $\overline{S}_i$ is the sensitivity index of parameter X_i, CWP_{xi} is the crop water productivity simulated by setting all parameters to default values, $CWP_{1.1xi}$ is the crop water productivity simulated by setting all parameters to default values except X_i, which is set to 110% of its default value, and $\mathrm{CWP}_{0.9xi}$ is the crop water productivity simulated by setting all parameters to default values except $\mathrm{X_i}$, which is set to 90% of its default value.

Five $\overline{S}_i$ values are first calculated in each grid cell corresponding to the five selected parameters. The parameter with the highest $\overline{S}_i$ is defined as the most sensitive parameter.

4. An illustration of the application of the GEPIC model

4.1. Case study and data sources

This study demonstrates the simulated CWP of wheat, maize, and rice at the global level in the year of 2000. These three crops accounted for about 76% of the global cereal harvested area and 86% of global cereal production in 2004 (FAO, 2006). The simulation is based on the crop distribution maps of these crops from Leff et al. (2004). The distribution maps have a spatial resolution of 30 arc-min (about 50 km × 50 km in each grid near the equator), and describe the fraction of a grid cell occupied by each of the crops. To determine whether crops are planted under rainfed or irrigated conditions, the irrigation map from Döll and Siebert (2000) was employed in combination with the crop distribution maps. When irrigation is equipped, all crops are assumed to be planted under irrigated conditions. Otherwise, they are categorized as being planted under rainfed conditions. Daily precipitation and daily maximum and minimum temperatures were collected for 11,729 meteorological stations from two sources: the Global Daily Climatology Network and the National Climate Data Center. Spatial distributed soil parameters were mainly derived from the Digital Soil Map of the World (FAO, 1990) and the International Soil Profile Data Set (Batjes, 1995). The amount of fertilizer applied per country and crop was derived from the international fertilizer industry association (IFA/IFDC/IPI/PPI/FAO, 2002).

4.2. Validation

There are several difficulties in validating the simulated results in this study. First, there are no high-resolution maps indicating spatial distribution of measured or statistical crop yield or CWP on a global scale. This makes grid-to-grid comparison between the simulated and statistical yields impossible. Second, although national statistics on crop yields are available from FAO (2006), few countries have reported national statistics on crop evapotranspiration or CWP. Considering the scarcely available data, the GEPIC model was validated in two ways. First, simulated national average yields, which were calculated based on the simulated crop yields and crop areas in each grid cell, were compared with the statistical national average yields from FAO (2006). Second, measured CWP values are often reported in literature for several agricultural experiment stations. These reported values were compared with the simulated CWP values in the grid cells where the stations are located.

It is worth noting that the crop distribution maps used in this paper are not completely consistent with FAO statistics. For instance, according to the crop distribution maps, rice is not planted in Algeria, but FAO has reported crop yield of rice there (although the total harvest area is lower than 200 ha in 2000 for the entire country). Here, only the countries where crop areas are reported in both the sources were compared, i.e. 102 countries for wheat, 124 countries for maize, and 103 countries for rice.

The comparison is shown in Fig. 3. The simulated yields and the statistical yields are quite comparable, as indicated by highly significant *F*-tests (the *P* values are all higher than 99%). For all the three crops, the trend lines are close to the 1:1 lines, and the R^2 values are higher than 0.6. Particularly for wheat, the R^2 value is almost 0.95. All the slopes of the trend lines are not significantly different from 1, while all the intercepts are not significantly different from 0. Considering the fact that this study uses default parameters in the EPIC model without conducting a model calibration (mainly due to the lack of measured or statistical data), the simulated results are regarded as very satisfactory for the three crops.

The simulated CWP at several sites was compared with the measured CWP as shown in Table 2. All the measured CWP values were obtained from a reviewer paper by Zwart and Bastiaanssen

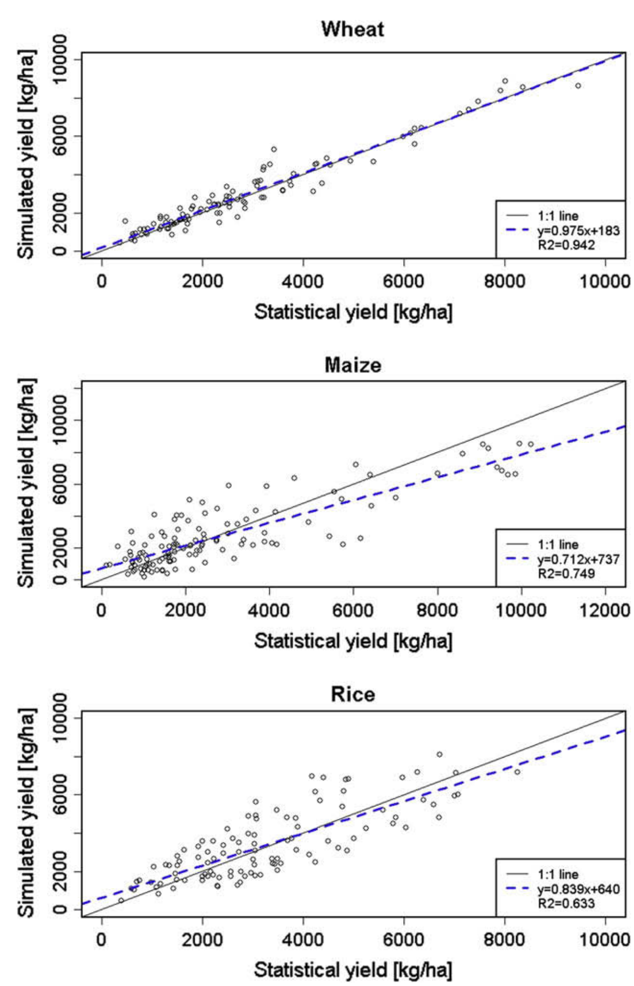

Fig. 3. Comparison between simulated yields and FAO statistical wheat yields in 2000.

Table 2
Comparison of the simulated CWP values with the measured CWP values

Location name	Measured CWP			Simulated CWP	Whether simulted CWP is within the range of the measured CWP
	Min kg/m^3	Max kg/m^3	Mean kg/m^3	kg/m^3	
Wheat					
Parana, Argentina	0.55	1.49	1.04	0.65	Yes
Merredin, Australia	0.56	1.14	0.95	0.82	Yes
Benerpota, Bangladesh	0.52	1.34	0.91	0.99	Yes
Quzhou, China	1.38	1.95	1.58	0.84	Yes
Xifeng, China	0.65	1.21	0.84	0.41	No
Luancheng, China	1.07	1.29	1.26	1.23	Yes
Yucheng, China	0.88	1.16	1.04	1.01	Yes
Beijing, China	0.92	1.55	1.19	1.23	Yes
West Bengal, India	1.11	1.29	1.19	0.87	No
Pantnagar, India	0.86	1.31	1.11	0.83	No
Karnal, India	0.27	0.82	0.67	0.49	Yes
Meknes, Morocco	0.11	1.15	0.58	0.48	Yes
Sidi El Aydi, Morocco	0.32	1.06	0.61	0.45	Yes
Faisalabad,Pakistan	0.7	2.19	1.28	0.70	Yes
Tel Hadya, Syria	0.48	1.1	0.78	0.56	Yes
Yellow Jacket (CO), USA	0.47	1.08	0.77	0.56	Yes
Grand Valley(CO), USA	1.53	2.42	1.72	0.96	No
Tashkent, Uzbekistan	0.44	1.02	0.73	0.75	Yes
Maize					
Azul, Argentina	1.84	2.79	2.35	1.33	No
Guaira, Brazil	1.13	1.33	1.21	1.73	No
Xifeng, China	1.26	2.31	2.00	1.94	Yes
Changwu, China	1.36	1.65	1.56	1.85	No
Yucheng, China	1.63	2.22	*1.93*	1.76	Yes
Luancheng, China	1.55	1.84	*1.70*	1.82	Yes
Pantnagar, India	1.17	1.74	1.47	1.44	Yes
Tal Amara, Lebanon	1.36	1.89	1.64	1.52	Yes
Sevilla, Spain	1.5	2.16	1.73	1.60	Yes
Szarvas, Hungary	1.28	2.44	1.85	1.30	Yes
Harran plain, Turkey	1.94	2.25	2.02	1.51	No
Cukurova, Turkey	0.22	1.25	1.01	1.73	No
Bushland, USA	0.89	1.74	*1.32*	1.49	Yes
Garden City, USA	0.83	1.68	1.26	1.51	Yes
Blacksburg, USA	1.34	3.26	2.67	1.82	Yes
Oakes, USA	2.03	2.86	2.55	2.16	Yes
Rice					
Zhanghe, China	1.04	2.2	1.41	1.18	Yes
Nanchang, China	1.63	2.04	1.84	1.88	Yes
Pantnagar, India	0.8	0.99	0.89	0.93	Yes
Raipur, India	0.46	0.82	0.46	0.46	Yes
New Delhi, India	0.55	0.67	0.67	0.33	No
Punjab, India	0.87	1.46	1.15	1.08	Yes
Muda, Malaysia	0.48	0.62	0.54	1.27	No
Kadawa, Nigeria	0.5	0.79	0.59	0.60	Yes
Luzon, Philippines	1.39	1.61	*1.50*	1.21	No
Beaumont, USA	1.37	1.44	*1.41*	1.39	Yes
Echuca, Australia	0.7	0.75	*0.73*	0.23	No

Sources: the measured CWP values are obtained from Zwart and Bastiaanssen (2004); the simulated CWP values are from this study.

(2004), who summarized the CWP values for wheat, maize and rice measured at different measurement stations in the past 25 years. The simulated CWP of wheat, maize and rice fell within the ranges of measured CWP at 82%, 67% and 64% of the locations, respectively. It needs to be pointed out that the CWP values reported by Zwart and Bastiaanssen represent irrigated agricultural systems. Since rainfed agriculture dominate Oceania and South America, it is not surprising that our simulated CWP values are much lower than the measured values at several sites in Argentina, Brazil and Australia.

There are very few measured CWP values reported for wheat, maize and rice for European countries in Zwart and Bastiaanssen's review paper. The author conducted an additional literature review and found that the CWP values have not been widely reported in Europe. Only a few values can be found in the literature, e.g. CWP of wheat in Italy (Van Hoorn et al., 1993; Katerji et al., 2005) and CWP of maize in France (Marty et al., 1975). Rice is not widely planted in Europe. For maize and wheat, the climatic conditions in many European countries are favorable for their production. In particular, in Western Europe, water is often not an important limiting factor for the growth of maize and wheat. Hence, in many European countries, increasing CWP may not be an issue as urgent as in other dry regions. This is possibly a reason for the few reports on CWP values there. In contrast, in the relatively dry regions (e.g. the North China Plain), water is a very limiting factor for crop growth. In addition, the use of water is competitive among agricultural and other sectors. In this situation, increasing CWP is a very important measure to guarantee high crop yield with limited water uses. The importance of improving CWP will likely result in more frequent reports on the CWP values in the literature in the dry regions such as the North China Plain.

According to the additional literature review, the CWP of wheat ranges from 1.02 to 1.59 kg m^{-3} in Italy (Van Hoorn et al., 1993; Katerji et al., 2005). In this study, the upper limit of simulated CWP of wheat is 1.52 kg m^{-3} in Italy, very close to the upper limit of 1.59 kg m^{-3} in the literature. The lower limit of the simulated CWP is 0.11 kg m^{-3}, and it is much smaller than the reported lower limit (i.e. 1.02 kg m^{-3}) in the literature. The smaller lower limit of this study is expected because this study covers all the cropland of wheat (based on the crop distribution maps), while the reported values are generally measured in specific locations. It is reasonable that our simulated values have a wider range of CWP. The measured CWP of maize is 1.6 kg m^{-3} in France (Marty et al., 1975), much smaller than the simulated national average CWP of maize of 2.19 kg m^{-3}. The measured value was based on experiments conducted in 1975, while our simulations represent the year of 2000. The crop yield of maize more than doubled between 1975 and 2000 (FAO, 2006); hence, much higher CWP values are expected in 2000 compared to those in 1975.

4.3. CWP

Simulation using the GEPIC model showed high spatial variation in the CWP of wheat, maize and rice in the year 2000 (Fig. 4). Table 3 shows the global and regional averages of CWP. The highest CWP of wheat occurs in Europe and Eastern Asia, while the lowest CWP occurs in Oceania and South America, where rainfed wheat dominates. The world average CWP of wheat is 0.952 kg m^{-3}. This number is close to but slightly lower than the mean CWP of wheat reported by Zwart and Bastiaanssen (2004) based on the measured CWP values (i.e. 1.09 kg m^{-3}). It is higher than that reported in Liu et al. (2007b) (i.e. 0.798 kg m^{-3}). Liu et al. do not use a crop distribution map for the simulation. Instead, they calculate the CWP values for all grid cells with dominant land-use of cropland and pasture. This simple treatment may be one reason for the lower value of world average CWP estimated in their study.

The regions with the highest CWP of maize are Western Europe, Eastern Asia, and North America, while the regions with the lowest CWP are Russia and Central Asia, and Eastern Africa. The world average CWP of maize is 1.425 kg m^{-3}. This value is lower than the mean CWP of maize calculated by Zwart and Bastiaanssen (2004) (i.e. 1.80 kg m^{-3}) mainly due to two reasons. First, Zwart and Bastiaanssen estimate the mean CWP of maize in absence of measured CWP values from Eastern Africa, Russia, and Central Asia, where the CWP of maize is generally lower than other regions. Second, Zwart and Bastiaanssen only reported CWP values for irrigated maize; hence, it is not surprising the derived world average CWP is higher.

Regions with the highest CWP of rice are Eastern Asia and North America, while regions with the lowest CWP are Oceania and Southern Africa. The world average CWP of rice is 1.046 kg m^{-3}, which is very close to the mean of CWP of rice calculated by Zwart and Bastiaanssen (2004) (i.e. 1.09 kg m^{-3}). Rice is often planted under irrigated conditions or under rainfed conditions with sufficient precipitation, e.g. in Southeast Asia. In light of this, the water stress of rice should be relatively low. Partly thanks to this, the simulated world average CWP of rice here is close to the one derived based on irrigated rice.

The CWP of maize (a C_4 crop) is generally higher than that of wheat and rice (C_3 crops) (Fig. 3). C_4 crops have roughly twice as high carbon assimilation per unit of transpiration compared with C_3 crops (Rockström, 2003). For a given climatic environment, C_4 crops are likely to be more efficient in assimilating carbon and obtaining higher crop yields with the same amount of water consumption. However, when comparing in different climate zones, it seems that the CWP of wheat in Western Europe is higher than the CWP of maize in many African countries (Fig. 4). CWP is determined not only by the carbon assimilation efficiency, but also the evaporative demand of the atmosphere or vapor pressure deficit. Many studies have reported inverse effects of vapor pressure deficit on CWP (Bierhuizen and Slayter, 1965; Zwart and Bastiaanssen, 2004). Tropical regions have a much higher vapor pressure deficit than temperate regions. The effect of vapor pressure deficit may compensate for or even exceeds the effect of the carbon assimilation efficiency, leading to possibly higher CWP of C_3 crops in temperate zones than that of C_4 crops in tropical zones.

4.4. Sensitivity analysis

The sensitivity index of the five parameters (WA, HI, PHU, PARM3 and PARM42) is first calculated for each grid cell for wheat, maize and rice. The parameter definitions are: WA is the energy conversion to biomass factor; HI is the potential harvest index for a crop under ideal growing conditions; PHU is the potential heat unit accumulation from emergence to maturity; PARM3 is the fraction of maturity when water stress starts reducing the harvest index; and PARM42 affects runoff thus soil water and ET. Then, the most sensitive parameter for CWP is selected for each grid cell and each crop (Fig. 5). The most sensitive parameter appears to vary among grid cells even for the same crop. For wheat, HI is the most sensitive parameter for CWP in 40% of the total grid cells. PARM42

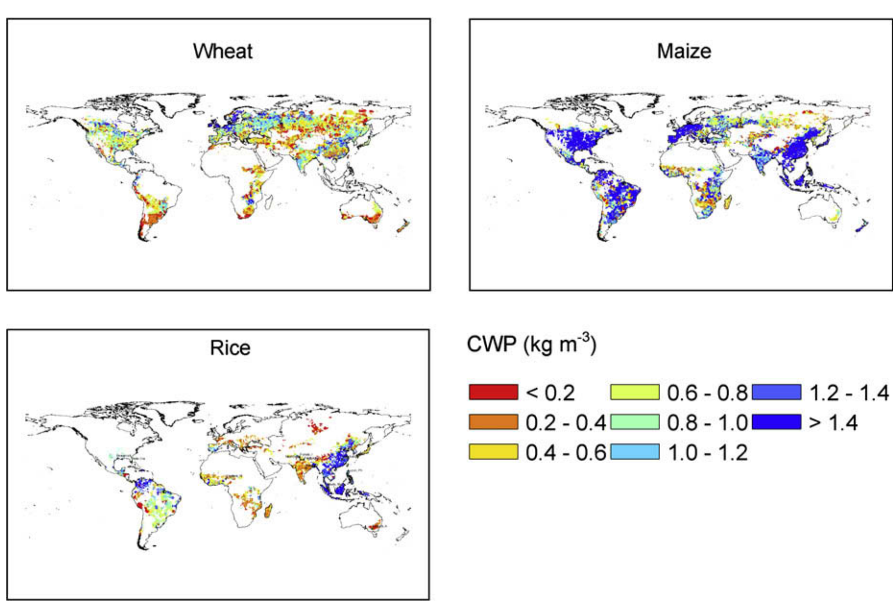

Fig. 4. Spatial distribution of crop water productivity of wheat, maize, and rice.

Table 3
Simulated regional average CWP for wheat, maize and rice

Region[a]	Wheat	Maize	Rice
S-SE-Asia	0.847	1.567	0.945
C-America	0.790	1.297	0.899
N-W-Africa	0.548	0.861	0.778
S-America	0.397	1.441	0.924
Oceania	0.370	1.312	0.227
E-Asia	1.125	1.706	1.345
Russia + C-Asia	0.977	0.693	0.345
W-Asia	0.650	1.391	0.440
N-America	0.901	1.582	1.066
W-Europe	1.256	1.796	0.701
E-Europe	1.102	0.862	0.462
W-Africa	0.691	1.010	0.529
S-Africa	0.404	0.884	0.283
E-Africa	0.578	0.778	0.474
World	0.930	1.425	1.046

[a] The regions are delimitated following that from Yang et al. (2006)

and WA, as the most sensitive parameters, account for 42% (23% for PARM42 and 19% for WA), while PARM3 and PHU together account for the remaining 18%. The CWP of maize is more sensitive to PHU, HI and WA than PARM3 and PARM42 in almost all grid cells. For maize, PHU, HI and WA, as the most sensitive parameters, each accounts for about one-third of the total grid cells (36% for PHU, 34% for HI and 29% for WA), while PARM3 and PARM42 are not the most sensitive parameters in almost all the grid cells. The results are consistent with the findings from Wang et al. (2005a), which concludes that crop yield or crop evapotranspiration is less sensitive to PARM3 and PARM42 for maize. For rice, HI is the most sensitive parameter in 64% of the grid cells, while WA and PHU are the most sensitive in 12% and 23% respectively. PARM3 and PARM42 are the most sensitive parameters in only 1% of the grid cells.

The five input parameters are ranked according to their influence on model output CWP at the continental level (Table 4). For wheat, HI is the most sensitive parameter in all continents. For maize, HI is the most sensitive parameter in Asia, Europe, South America and Oceania, but WA is the most sensitive one in North America and Africa (in both the continents, HI is the second most sensitive parameter). The results also show that, for maize, PARM3 and PARM42 are the least sensitive among the five parameters. For rice, HI and WA are always the first and second most sensitive parameters in all continents, except for Oceania. In Oceania, WA is the most sensitive parameter for CWP, while HI is the second most sensitive one.

Crop yield has a linear relation to HI in the absence of water stress. This relation leads to frequent high sensitivity of CWP to HI. When water stress occurs, the actual harvest index may be much lower than HI which reduces HI sensitivity. Water stress is generally high under rainfed conditions in dry regions. This may be a reason that HI is not the most sensitive parameter for the CWP of maize in Africa. Biomass production is linearly related to WA under non-stressed conditions. However, biomass may be greatly reduced if the crop is stressed, thus reducing WA sensitivity. Crop yield can be sensitive to PHU because PHU sets the time scale (expressed in temperature rather than time). Short PHU values give rapid early growth but less total time to convert energy to biomass. Thus, the sensitivity to PHU depends on several factors with weather being the most important. Since PARM3 sets the time when water stress starts affecting harvest index, crop yield may be affected but the sensitivity is usually not large over a narrow range. PARM42 is

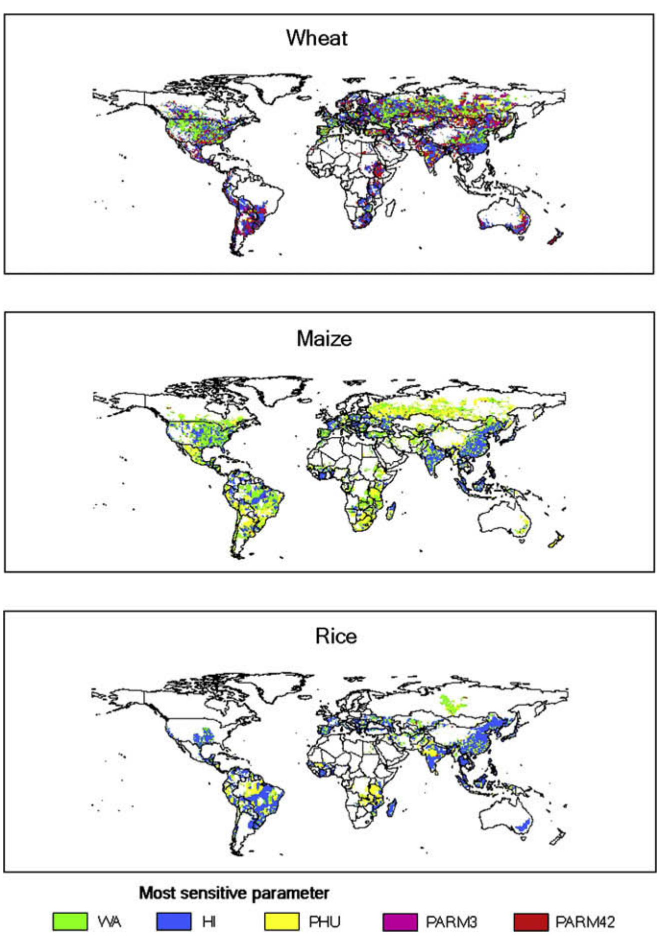

Fig. 5. The most sensitive parameter for wheat, maize and rice.

Table 4
Sensitivities of CWP of wheat, maize and rice to five parameters at the continental level

Continent	Parameter	Wheat		Maize		Rice	
		$\bar{S}_i$	Rank	$\bar{S}_i$	Rank	$\bar{S}_i$	Rank
Asia	WA	0.215	5	0.345	3	0.485	2
	HI	0.995	1	1.012	1	0.997	1
	PHU	0.505	2	0.483	2	0.318	5
	PARM3	0.270	3	0.009	5	0.334	4
	PARM42	0.252	4	0.010	4	0.342	3
North America	WA	0.640	2	0.566	1	0.643	2
	HI	0.736	1	0.510	2	0.972	1
	PHU	0.353	3	0.400	3	0.133	5
	PARM3	0.256	5	0.019	4	0.285	3
	PARM42	0.258	4	0.005	5	0.284	4
Europe	WA	0.222	5	0.560	2	0.771	2
	HI	1.257	1	0.730	1	0.962	1
	PHU	0.962	2	0.364	3	0.173	3
	PARM3	0.706	3	0.050	4	0.112	5
	PARM42	0.682	4	0.010	5	0.120	4
Africa	WA	0.359	5	0.532	1	0.592	2
	HI	1.062	1	0.394	2	0.971	1
	PHU	0.636	2	0.283	3	0.229	3
	PARM3	0.548	3	0.033	4	0.172	5
	PARM42	0.531	4	0.020	5	0.190	4
South America	WA	0.404	2	0.463	3	0.692	2
	HI	0.482	1	0.592	1	0.932	1
	PHU	0.156	3	0.476	2	0.387	3
	PARM3	0.142	4	0.045	4	0.097	5
	PARM42	0.127	5	0.018	5	0.109	4
Oceania	WA	0.595	2	0.169	2	0.790	1
	HI	0.700	1	0.203	1	0.648	2
	PHU	0.210	4	0.126	3	0.291	3
	PARM3	0.205	5	0.009	5	0.098	5
	PARM42	0.217	3	0.039	4	0.102	4

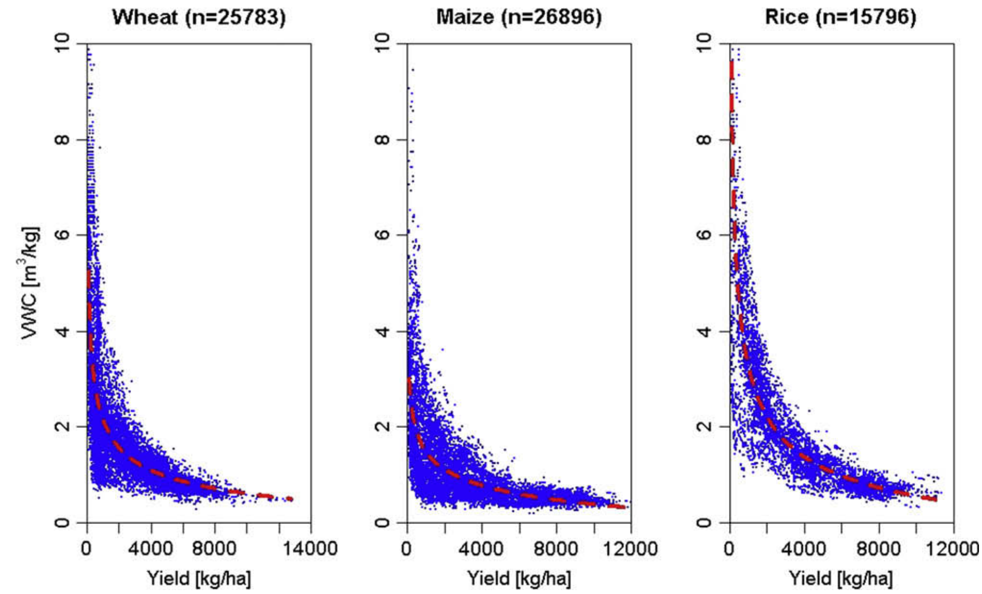

Fig. 6. The relation between VWC and crop yield for all calculated grid cells (total number of *n*).

non-linearly related to runoff so it affects soil water and thus ET and crop growth. In general, CWP is more sensitive to HI, WA and PHU than PARM3 and PARM42 (Table 4). This is because HI, WA and PHU have a more direct relation to crop yield than PARM3 and PARM42.

4.5. VWC – yield relation

Many authors have reported a linear relationship between crop yield and seasonal ET (Zhang and Oweis, 1999; Huang et al., 2004). The linear ET-yield relationship leads to a constant CWP, or constant VWC. Our results show a non-linear inverse relationship between VWC and yield (Fig. 6). VWC decreases with the increase of crop yield. Obviously, the results do not support the linear ET-yield relationship. ET includes two components: productive crop transpiration (T), which is closely related to crop growth and crop yield, and unproductive soil evaporation (E), which does not contribute to crop growth. In addition, E tends to decrease with a higher yield as a result of shading from increased leaf area (Rockström and Barron, 2007). The linear relationship between ET and crop yield may exist for specific crop growth stages, but this relationship is obviously too simplified for the entire growth period.

The results support the findings suggesting that a linear relationship between yield and ET does not apply, especially for the low yield ranges (e.g. $<6000\ \mathrm{kg\ ha^{-1}}$ for wheat and maize and $<8000\ \mathrm{kg\ ha^{-1}}$ for rice) (see Fig. 6). The non-linear ET-yield relations have been reported in other literature (Falkenmark and Rockström, 2004; Oweis and Hachum, 2006).

Low crop yield may be caused by water stress in sensitive crop growth stages. The water stress reduces crop yield substantially, but may affect ET in other stages less. Hence, ET in the entire growth period will not be reduced linearly with the yield reduction, leading to high VWC values and low CWP values. The VWC-yield relation has important implications for water resources management. The low yield with high VWC (or low CWP) often exists in rainfed conditions in a dry environment, e.g. in many smallholder farms in Africa. When crop yield is low, e.g. <3 kg/ha, supplemental irrigation can significantly improve crop yield, but may only slightly increase seasonal ET. The result is a decreasing VWC, or increasing CWP.

5. Conclusion

GEPIC provides an effective tool to estimate crop water productivity (CWP) on a global scale with high spatial resolutions. The simulation results from the GEPIC model allow broader applications of the database of CWP of wheat, rice and maize. Moreover, the GEPIC model provides a systematic and flexible tool to study crop-water relations on different geographical scales with flexible spatial resolutions. The model allows users to specify the study area and spatial resolution based on their own needs and purposes.

The GEPIC model connects the entire EPIC model with a GIS. Hence, it can go beyond the study of crop-water relations. For instance, the EPIC model also simulates crop growth based on climate parameters such as precipitation and temperature, and nutrient budgets. The GEPIC model thus has the potential to be applied to study the impacts of global climate change on food production, and changes in nutrient dynamics by (increased) agricultural activities. These two areas are emphasized in the ongoing research in our research group.

The accuracy of the GEPIC output depends largely on the quality of the input data. So far, detailed information on crop parameters, crop calendar, and irrigation and fertilizer application for specific crops is not available on a global scale. Assumptions have to be made when using the GEPIC model due to the insufficient input data. The default crop parameters are used for all the regions, but they cannot exactly reflect the local crop characteristics. Access to the more detailed data sets will improve the accuracy of the simulation results. However, as long as the database on these factors is weak, the possibility of reducing uncertainty remains limited. Based on personal experience, the following high-resolution data are needed to fully exploit the potential of GEPIC: irrigation depth, fertilizer application rate, crop calendar, and up-to-date land-use data.

Without high-resolution data on crop yield or CWP, it is difficult to assess the accuracy of the GEPIC model at the grid cell level. Here a qualitative assessment is conducted. The simulation results show that highest yield of wheat occurs in grid cells located in Europe and Eastern Asia, highest yield of maize occurs in grid cells located in Western Europe, Eastern Asia, Southeast Asia, and North America, while highest yield of rice occurs in grid cells located in Eastern Asia, Southeast Asia and Northern part of South America (the results are not presented in the paper). The results are consistent with the statistical yield data of these three crops from FAO (2006). The consistence indicates that the GEPIC model is able to generate a reliable distribution pattern of crop yield at the grid cell level (as well as CWP considering the close relationship between CWP and crop yield).

The comparison between the simulated CWP values in several grid cells with the measured CWP values located within the grid cells (Table 2) shows a general underestimation of CWP in the sites where a large amount of fertilizer is applied, e.g. Xifeng and Luancheng in China, West Bengal and Pantnagar in India and Grand Valley in USA etc. CWP is greatly affected by the application rate of fertilizer, particularly nitrogen fertilizer (Liu et al., 2007b); while in this study, the national average fertilizer application rate is used for all grid cells within a country. This assumption likely leads to underestimation of CWP in the regions with higher fertilizer application rates than the country average, and overestimation of CWP in the regions with lower fertilizer application rates. The assumption of even distribution of fertilizer application rates within a country is a compromise for the absence of the high-resolution fertilizer data, but this assumption is in my opinion the most important source of the simulation errors at the grid cell levels.

Another major source of error is the irrigation map. Although high-resolution irrigation map is available, crop-specific irrigation map is absent. It is assumed that all crops are planted under irrigated conditions when irrigation is equipped. This assumption may be sound for rice and wheat, since both the crops rely heavily on irrigation. However, it may overestimate crop yield as well as CWP of maize in large areas (e.g. in the southern part of China where rainfed maize is often practiced but irrigation is also equipped according to the irrigation map). The lack of crop-specific irrigation map is a constraint for global studies on food production and agricultural water use, and this limitation has been realized by the scientific community. The third major source is the uncertainty of three crop parameters, i.e. potential harvest index, energy-biomass conversion ratio, and potential heat unit, as shown in the sensitivity analysis in this paper. Collection of these parameters with a high spatial resolution seems difficult in the near future in light of the rare report on them. One possible solution is to estimate them with a calibration process, which requires high-resolution data on crop yield. Hence, collection of crop yield data with a high-resolution, or even at a sub-national level, will help reduce the uncertainty caused by these parameters.

The GEPIC model mainly focuses on the natural, physical, and management factors influencing crop production. There is insufficient emphasis on the economic aspects. The GEPIC model considers technological advances as an influencing factor for crop yield, and associates them with the harvest index of individual crops. However, it is not possible to directly study the effects of various food policies and agricultural research investment on crop production. To take these economic issues into account, the economic component in the GEPIC model needs further development.

In this paper, the OAT approach for sensitivity analysis is applied rather mechanistically by adjusting the parameters by $\pm 10\%$. This kind of sensitivity analysis does not take into account the difference between the parameters. The application of this approach is mainly a compromise for the high computation cost of the sampling-based sensitivity analysis. A further improvement in computer speed in the future will make sampling-based sensitivity analysis possible for this study. Currently, a sampling-based sensitivity analysis may only be feasible for a small region, e.g. North China Plain, but it is very challenging on a large scale.

Acknowledgements

This study was supported by the Swiss National Science Foundation (Project No: 205121-103600), and the European Commission within the GEO-BENE project framework (Global Earth Observation – Benefit Estimation: Now, Next and Emerging, Proposal No. 037063). I thank Prof. Alexander J.B. Zehnder (Board of the Swiss Federal Institutes of Technology), Dr. Hong Yang and Dr. Juergen Schuol (Swiss Federal Institute of Aquatic Science and Technology) and Dr. Jimmy R. Williams (Texas Agricultural Experiment Station) for their valuable comments and suggestions. Thanks should also be given to Prof. Tony Jakeman, Prof. Ari Jolma and the three anonymous reviewers for their constructive comments on the earlier version of the manuscript. Any remaining errors are solely the author's responsibility.

References

Batjes, N.H., 1995. A Homogenized Soil Data File for Global Environmental Research: a Subset of FAO. Working Paper and Preprint 95/10b. International Soil Reference and Information Center, Wageningen, the Netherlands.
Bierhuizen, J.F., Slayter, R.O., 1965. Effect of atmospheric concentration of water vapour and CO2 in determining transpiration–photosynthesis relationships of cotton leaves. Agricultural Meteorology 2, 259–270.
Brunner, A.C., Park, S.J., Ruecker, G.R., Dikau, R., Vlek, P.L.G., 2004. Catenary soil development influencing erosion susceptibility along a hillslope in Uganda. CATENA 58 (1), 1–22.
Burt, J.E., Hayes, J.T., O'Rourke, P.A., Terjung, W.H., Tod-hunter, P.E., 1981. A parametric crop water use model. Water Resources Research 17, 1095–1108.
Campolongo, F., Cariboni, J., Saltelli, A., 2007. An effective screening design for sensitivity analysis of large models. Environmental Modelling and Software 22 (10), 1509.
Clarke, D., Smith, M., El-Askari, K., 1998. CropWat for Windows: User Guide, Version 4.2. Food and Agriculture Organization of the United Nations, Rome.
Curry, R.B., Peart, R.M., Jones, J.W., Boote, K.J., Allen, L.H., 1990. Simulation as a tool for analyzing crop response to climate change. Transactions of the ASAE 33 (3), 981–990.
Döll, P., Siebert, S., 2000. A digital global map of irrigated areas. ICID Journal 49 (2), 55–66.
Doos, B.R., Shaw, R., 1999. Can we predict the future food production? A sensitivity analysis. Global Environmental Change 9 (4), 261–283.
Dyson, T., 1996. Population and Food: Global Trends and Future Prospects. Routledge, London and New York.
Dyson, T., 1999. World food trends and prospects to 2025. Proceedings of the National Academy of Sciences of the United States of America 96, 5929–5936.
ESRI, 2004. ArcGIS Desktop Developer Guide ArcGIS 9. ESRI Press, Redlands, California.
Evans, L.T., 1998. Feeding the Ten Billion. Plants and Population Growth. Cambridge University Press, Cambridge, UK.
Falkenmark, M., Rockström, J., 2004. Balancing Water for Humans and Nature. Earthscan, London.
FAO, 1990. Soil units of the soil map of the world. In: FAO-UNESCO-ISRIC, Rome, Italy.
FAO, 2006. FAOSTAT: FAO statistical databases. In: Food and Agriculture Organization of the United Nations, Rome.
Fischer, G., van Velthuizen, H.T., Shah, M., Nachtergaele, F.O., 2002. Global Agro-Ecological Assessment for Agriculture in the 21st Century: Methodology and Results. IIASA Research Report RR-02–002. International Institute for Applied Systems Analysis, Laxenburg, Austria.
Frohberg, H., Britz, W., 1994. The World Food Model and an Assessment of the impact of the GATT agreement on Agriculture. Research report, Bonn, Germany.
Gimenez, C., Mitchell, V.J., Lawlor, D.W., 1992. Regulation of photosynthetic rate of 2 sunflower hybrids under water-stress. Plant Physiology 98 (2), 516–524.
Hargreaves, G.H., Samani, Z.A., 1985. Reference crop evapotranspiration from temperature. Applied Engineering in Agriculture 1, 96–99.
Hijmans, R.J., Guiking-Lens, I.M., van Diepen, C.A., 1994. WOFOST 6.0. (user's guide for the WOFOST 6.0 crop growth simulation model). Technical Document 12 DLO Winand Staring Centre, Wageningen.
Hoekstra, A.Y., Hung, P.Q., 2005. Globalisation of water resources: international virtual water flows in relation to crop trade. Global Environmental Change Part A 15 (1), 45–56.
Holbrook, N.M., Zwieniecki, M.A., 2003. Water gate. Nature 425, 361.
Huang, M., Gallichand, J., Zhong, L., 2004. Water-yield relationships and optimal water management for winter wheat in the Loess Plateau of China. Irrigation Science 23 (2), 47–54.
IBSNAT, 1989. Decision Support System for Agrotechnology Transfer V2.10 (DSSAT V2.10). Honolulu: Department of Agronomy and Soil Science. College of Tropical Agriculture and Human Resources: University of Hawaii, Hawaii.
IFA/IFDC/IPI/PPI/FAO, 2002. Fertilizer Use by Crops, fifth ed. International Fertilizer Industry Association, Rome.
Iglesias, A., Rosenzweig, C., Pereira, D., 2000. Agricultural impacts of climate change in Spain: developing tools for a spatial analysis. Global Environmental Change-Human and Policy Dimensions 10 (1), 69–80.
Ines, A.V.M., Gupta, A.D., Loof, R., 2002. Application of GIS and crop growth models in estimating water productivity. Agricultural Water Management 54 (3), 205–225.

Katerji, N., Van Hoorn, J.W., Hamdy, A., Mastrorilli, M., Nachit, M.M., Oweis, T., 2005. Salt tolerance analysis of chickpea, faba bean and durum wheat varieties: II. Durum wheat. Agricultural Water Management 72 (3), 195.
Lauer, M.J., Boyer, J.S., 1992. Internal CO_2 measured directly in leaves – abscisic-acid and low leaf water potential cause opposing effects. Plant Physiology 98 (4), 1310–1316.
Lawlor, D., 1995. The effects of water deficit on photosynthesis. In: Smirnoff, N. (Ed.), Environment and Plant Metabolism. Flexibility and Acclimation. BIOS Scientific Publishers, Oxford, UK.
Leff, B., Ramankutty, N., Foley, J.A., 2004. Geographic distribution of major crops across the world. Global Biogeochemical Cycles 18 (1), GB1009.
Liu, J., Wiberg, D., Zehnder, A.J.B., Yang, H., 2007a. Modelling the role of irrigation in winter wheat yield, crop water productivity, and production in China. Irrigation Science 26 (1), 21–33.
Liu, J., Williams, J.R., Zehnder, A.J.B., Yang, H., 2007b. GEPIC – modelling wheat yield and crop water productivity with high resolution on a global scale. Agricultural Systems 94 (2), 478–493.
Marty, J.R., Puech, J., Maertens, C., Blanchet, R., 1975. Etude expérimentale de la réponse de quelques grandes cultures à l'irrigation. Comptes Rendus de l'Academie d'Agriculture de France 61, 560–567.
McCuen, R.H., 1973. Role of sensitivity analysis in hydrologic modeling. Journal of Hydrology 18 (1), 37.
Monsi, M., Saeki, T., 1953. Uber den Lichfaktor in den pflanzengesells chaften und seine bedeutung fuer die stoffproduktion. Japanese Journal of Biotechnology 14, 22–52.
Monteith, J.L., 1977. Climate and the efficiency of crop production in Britain. Philosophical Transactions of the Royal Society B 281, 277–294.
Norton, J.P., 2008. Algebraic sensitivity analysis of environmental models. Environmental Modelling and Software 23 (8), 963.
Ort, D.R., Oxborough, K., Wise, R.R., 1994. Depressions of photosynthesis in crops with water defecits. Photoinhibition of Photosynthesis – from Molecular Mechanisms to the Field. In: Bowyer, J., Baker, N.R. (Eds.), Photoinhibition of Photosynthesis. Bios Scientific Publishers, Oxford, UK.
Oweis, T., Hachum, A., 2006. Water harvesting and supplemental irrigation for improved water productivity of dry farming systems in West Asia and North Africa. Agricultural Water Management 80, 1–3. 57.
Parry, M., Rosenzweig, C., Iglesias, A., Fischer, G., Livermore, M., 1999. Climate change and world food security: a new assessment. Global Environmental Change 9 (Suppl. 1), S51–S67.
Parton, W.J., McKeown, B., Kirchner, V., Ojima, D.S., 1992. CENTURY Users' Manual. Colorado State University, NREL Publication, Fort Collins, Colorado, USA.
Priya, S., Shibasaki, R., 2001. National spatial crop yield simulation using GIS-based crop production model. Ecological Modelling 136, 2–3. 113.
Quick, W.P., Chaves, M.M., Wendler, R., David, M., Rodrigues, M.L., Passaharinho, J.A., Pereira, J.S., Adcock, M.D., Leegood, R.C., Stitt, M., 1992. The effect of water-stress on photosynthetic carbon metabolism in 4 species grown under field conditions. Plant Cell and Environment 15 (1), 25–35.
Rao, M.N., Waits, D.A., Neilsen, M.L., 2000. A GIS-based modeling approach for implementation of sustainable farm management practices. Environmental Modelling & Software 15 (8), 745–753.
Ritchie, J.T., 1972. A model for predicting evaporation from a row crop with incomplete cover. Water Resources Research 8, 1204–1213.
Rockström, J., 2003. Water for food and nature in drought-prone tropics: vapour shift in rain-fed agriculture. Philosophical Transactions of the Royal Society of London B Biological Sciences 358 (1440), 1997–2009.
Rockström, J., Barron, J., 2007. Water productivity in rainfed systems: overview of challenges and analysis of opportunities in water scarcity prone savannahs. Irrigation Science 25 (3), 299–311.
Rockström, J., Lannerstad, M., Falkenmark, M., 2007. Assessing the water challenge of a new green revolution in developing countries. Proceedings of the National Academy of Sciences of the United States of America 104 (15), 6253–6260.
Rosegrant, M., Cai, X., Cline, S., 2002. World Water and Food to 2025: Dealing with Scarcity. International Food Policy Research Institute, Washington DC.
Rosegrant, M.W., Paisner, M.S., Meijer, S., Witcover, J., 2001. Global Food Projections to 2020 – Emerging Trends and Alternative Futures. International Food Policy Research Institute, Washington, DC.
Rosenzweig, C., Iglesias, A., 1998. The use of crop models for international climate change impact assessment. In: Tsuji, G.Y., Hoogenboom, G., Thornton, P.K. (Eds.), Understanding Options for Agricultural Production. Kluwer Academic Publishers, Dordrecht.
Rosenzweig, C., Iglesias, A., Fischer, G., Liu, Y., Baethgen, W., Jones, J.W., 1999. Wheat yield functions for analysis of land-use change in China. Environmental Modeling and Assessment 4, 115–132.
Seckler, D., Amarasinghe, U., Molden, D.J., de Silva, R., Barker, R., 1998. World Water Demand and Supply, 1990 to 2025: Scenarios and Issues. IWMI, Colombo, Sri Lanka.
Stevens, D., Dragicevic, S., Rothley, K., 2007. iCity: a GIS-CA modelling tool for urban planning and decision making. Environmental Modelling & Software 22 (6), 761–773.
Stockle, C.O., Donatelli, M., Nelson, R., 2003. CropSyst, a cropping systems simulation model. European Journal of Agronomy 18 (3–4), 289–307.
Stockle, C.O., Martin, S.A., Campbell, G.S., 1994. Cropsyst, a cropping systems simulation-model – water nitrogen budgets and crop yield. Agricultural Systems 46 (3), 335–359.
Tan, G., Shibasaki, R., 2003. Global estimation of crop productivity and the impacts of global warming by GIS and EPIC integration. Ecological Modelling 168 (3), 357.
Tezara, W., Mitchell, V.J., Driscoll, S.D., Lawlor, D.W., 1999. Water stress inhibits plant photosynthesis by decreasing coupling factor and ATP. Nature 401, 914–917.
Tweeten, L., 1998. Anticipating a tighter global food supply-demand balance in the 21st century. Choices 3, 8–12.
Van Hoorn, J.W., Katerji, N., Hamdy, A., Mastrorilli, M., 1993. Effect of saline water on soil salinity and on water stress, growth, and yield of wheat and potatoes. Agricultural Water Management 23 (3), 247.
Wang, X., He, X., Williams, J.R., Izaurralde, R.C., Atwood, J.D., 2005a. Sensitivity and uncertainty analyses of crop yields and soil organic carbon simulated with EPIC. Transactions of the ASAE 48 (3), 1041–1054.
Wang, X., Youssef, M.A., Skaggs, R.W., Atwood, J.D., Frankenberger, J.R., 2005b. Sensitivity analyses of the nitrogen simulation model, DRAINMOD-N II. Transactions of the American Society of Agricultural Engineers 48 (6), 2205.
Williams, J.R., Jones, C.A., Kiniry, J.R., Spanel, D.A., 1989. The EPIC crop growth model. Transactions of the ASAE 32, 497–511.
Yang, H., Wang, L., Abbaspour, K.C., Zehnder, A.J.B., 2006. Virtual water trade: an assessment of water use efficiency in the international food trade. Hydrology and Earth System Sciences 10, 443–454.
Zhang, H., Oweis, T., 1999. Water-yield relations and optimal irrigation scheduling of wheat in the Mediterranean region. Agricultural Water Management 38 (3), 195–211.
Zwart, S.J., Bastiaanssen, W.G.M., 2004. Review of measured crop water productivity values for irrigated wheat, rice, cotton and maize. Agricultural Water Management 69 (2), 115–133.

Junguo Liu is a post-doc scientist at the Swiss Federal Institute of Aquatic Science and Technology (Eawag). His research interest focuses on global water scarcity, global water–food relations, global nutrient cycle, global virtual water trade, and the impacts of climate change on global water and food systems.